IOP Publishing Phys. Med. Biol. 63 (2018) 055001 (17pp) https://doi.org/10.1088/1361-6560/aaac23

Physics in Medicine & Biology

IPEM Institute of Physics and Engineering in Medicine

PAPER

End-to-end tests using alanine dosimetry in scanned proton beams

A Carlino[1,3], C Gouldstone[2], G Kragl[1], E Traneus[4], M Marrale[3], S Vatnitsky[1], M Stock[1] and H Palmans[1,2]

[1] EBG MedAustron GmbH, Marie Curie-Straße 5, A-2700 Wiener Neustadt, Austria
[2] National Physical Laboratory, Hampton Road, TW11 0LW Teddington, United Kingdom
[3] Department of Physics and Chemistry, University of Palermo, Viale delle Scienze, Edificio 18, 90128 Palermo, Italy
[4] RaySearch Laboratories AB, Sveavägen 44, PO Box 3297, Stockholm, Sweden

E-mail: antonio.carlino@medaustron.at

RECEIVED
16 August 2017

REVISED
26 January 2018

ACCEPTED FOR PUBLICATION
31 January 2018

PUBLISHED
26 February 2018

Keywords: protons, alanine, audit, dosimetry, anthropomorphic phantoms, end to end test

Abstract

This paper describes end-to-end test procedures as the last fundamental step of medical commissioning before starting clinical operation of the MedAustron synchrotron-based pencil beam scanning (PBS) therapy facility with protons.

One in-house homogeneous phantom and two anthropomorphic heterogeneous (head and pelvis) phantoms were used for end-to-end tests at MedAustron. The phantoms were equipped with alanine detectors, radiochromic films and ionization chambers. The correction for the 'quenching' effect of alanine pellets was implemented in the Monte Carlo platform of the evaluation version of RayStation TPS. During the end-to-end tests, the phantoms were transferred through the workflow like real patients to simulate the entire clinical workflow: immobilization, imaging, treatment planning and dose delivery. Different clinical scenarios of increasing complexity were simulated: delivery of a single beam, two oblique beams without and with range shifter. In addition to the dose comparison in the plastic phantoms the dose obtained from alanine pellet readings was compared with the dose determined with the Farmer ionization chamber in water.

A consistent systematic deviation of about 2% was found between alanine dosimetry and the ionization chamber dosimetry in water and plastic materials. Acceptable agreement of planned and delivered doses was observed together with consistent and reproducible results of the end-to-end testing performed with different dosimetric techniques (alanine detectors, ionization chambers and EBT3 radiochromic films).

The results confirmed the adequate implementation and integration of the new PBS technology at MedAustron. This work demonstrates that alanine pellets are suitable detectors for end-to-end tests in proton beam therapy and the developed procedures with customized anthropomorphic phantoms can be used to support implementation of PBS technology in clinical practice.

1. Introduction

Light ion beam therapy (LIBT) represents an irradiation technique taking full advantage of the physical interaction properties of light ions with tissues and an advanced delivery modality. LIBT with scanned beams generates highly conformal treatments with the potential of very sharp gradients in 3 dimensions, with many degrees of freedom available at the planning level. Formalisms of absorbed dose-to-water determination based on ^{60}Co calibration coefficients in water was implemented into dosimetry practice of radiotherapy with high-energy photon and electron beams within the last two decades. Same formalisms have also been applied for protons and heavier ions using ionization chambers calibrated in a ^{60}Co beam as the main reference dosimetry technique (International Atomic Energy Agency 2000). However, the lack of international and national primary dosimetry standards for light ion beams complicated the implementation of a consistent approach to harmonize different beam modalities (e.g. photon versus ion beam therapy). Combined with a lack of international guidelines and consensus on calibration methods for scanned beams (Palmans and Vatnitsky 2016) this results in larger uncertainties in comparison to photons and also potential impact on uncertainty in biological data (relative biological effectiveness, RBE). In order to evaluate beam monitor calibration methods several reference

dosimetry intercomparisons for proton and carbon ion beams were performed (Fukumura *et al* 1998, Vatnitsky *et al* 1999, Moyers *et al* 2014, Bäumer *et al* 2017). Such comparison studies are extremely useful, especially for new facilities, to detect and eliminate any possible systematic errors occurring during beam calibration process. Reference dosimetry intercomparisons are, however, not sufficient to ensure accurate clinical doses in scanned LIBT given the complexity of dose delivery resulting from the simultaneous optimization of a large number of beamlet weights. As part of a comprehensive approach to quality assurance, an independent external dosimetry audit is desirable (Clark *et al* 2009, 2014, Eaton *et al* 2017).

The purpose of such audits is to achieve sufficient dosimetric accuracy among the participating radiotherapy centers and to ensure the comparability and reproducibility of clinical studies and treatment protocols. As an independent audit has not yet been established for LIBT facilities, the most efficient solution for validation of new beam delivery technology is to perform so-called end-to-end test. The purpose of end-to-end testing is to confirm that the entire logistic chain of a radiation treatment starting from CT imaging, treatment planning, monitor calibration, patient positioning and verification and beam delivery is adequately implemented resulting in sufficient accuracy of planned dose delivery. Before starting the treatment of tumor sites in a new body region, a full simulation of the workflow should be performed that includes every step of the treatment process when the phantoms of different level of sophistication are moved along the workflow like real patients. Highly advanced auditing procedures and end-to-end tests with homogeneous or heterogeneous anthropomorphic phantoms on advanced treatment techniques, have been established by the imaging and radiation oncology core (IROC) (Ibbott *et al* 2008). The IROC is auditing proton facilities in the US using optical stimulated luminescence dosimeters (Aguirre *et al* 2009, Kerns *et al* 2012) and thermoluminescence dosimeters. Contrary to the latter, for which the correction factors for quenching in scanning proton and carbon beams are not accurately known, previous studies showed the feasibility of alanine electron paramagnetic resonance (EPR) dosimetry in Ion beam therapy (Herrmann *et al* 2011, Ableitinger *et al* 2013, Marrale *et al* 2016). Moreover, dosimetric audits to verify the dosimetric accuracy of conventional photon and electron beams for IMRT with alanine detectors are well established in Belgium (Schaeken *et al* 2011) and the UK (Budgell *et al* 2011). A strong motivation to use alanine as dosimeter for end-to-end tests is a very stable post-irradiation signal and the non-destructive readout process which make them suitable for archiving and possible future analysis (contrarily to thermoluminescence technique where the readout deletes the stored dose information). Alanine detectors exhibit a linear dose response up to high dose levels of about 10^5 Gy and they are dose-rate independent up to extremely high dose rates. The latter is a very favorable feature in scanning beams with high local and instantaneous dose rates. Alanine detectors were proposed and provided for this study by the National Physical Laboratory (NPL) for measurements in proton beams (Palmans 2003). The response of alanine detectors depends on the particle-energy spectrum and requires therefore specific correction factors (Hansen and Olsen 1985) that were computed based on a research version of the RayStation (Saini *et al* 2016) treatment planning system (TPS).

This paper describes end-to-end test procedures implemented as the last fundamental step of medical commissioning before starting clinical operation of a synchrotron-based scanning beam therapy facility with protons. MedAustron is equipped with a synchrotron facility able to accelerate ions from protons up to Neon for medical and research purpose. The facility can deliver protons with kinetic energies from 62 to 252 MeV (ranges from 3 to 38 cm in water). This work can be seen as the further development of the feasibility study for dosimetric auditing procedures at LIBT facilities reported by Ableitinger *et al* (2013). The procedures described in the current paper are focused only on the physical dose delivery in scanned proton beams. Any possible validation of the RBE-weighted proton absorbed dose (International Commission on Radiation Units and Measurements 2007) is out of the scope of this work.

2. Materials and methods

2.1. Phantoms

In order to perform the end-to-end tests at MedAustron one homogeneous phantom and two anthropomorphic phantoms (head and pelvis) were customized. The homogenous polystyrene phantom was previously used to test the feasibility of an audit procedure with protons and carbon ions at the HIT facility (Ableitinger *et al* 2013). The mass density was close to water. The phantom was designed in a way that its dimensions represent the size of a head. Seven plates, each with a size of $20 \times 20 \times 3\,cm^3$, were stacked together to form a 21 cm long phantom. The phantom can host a set of 20 alanine pellets that were arranged in a specific pattern that minimized the shadowing of the detectors in the Beam's eye view. In addition to the cavities for the alanine pellets, two radiochromic films can be placed just upon the pellets and perpendicular to the beam direction. In this way the 'quenching' effect on the film is minimized (Martišíková *et al* 2008, Martišíková and Jäkel 2010). Moreover, the phantom can allocate different inserts for ionisation chambers (Farmer $0.6\,cm^3$ TM30013 and Semiflex $0.3\,cm^3$ TM31013). White marking lines on the surface of the assembled phantom allow an accurate alignment at the planning CT and at the robotic treatment couch with in-room lasers in the irradiation room.

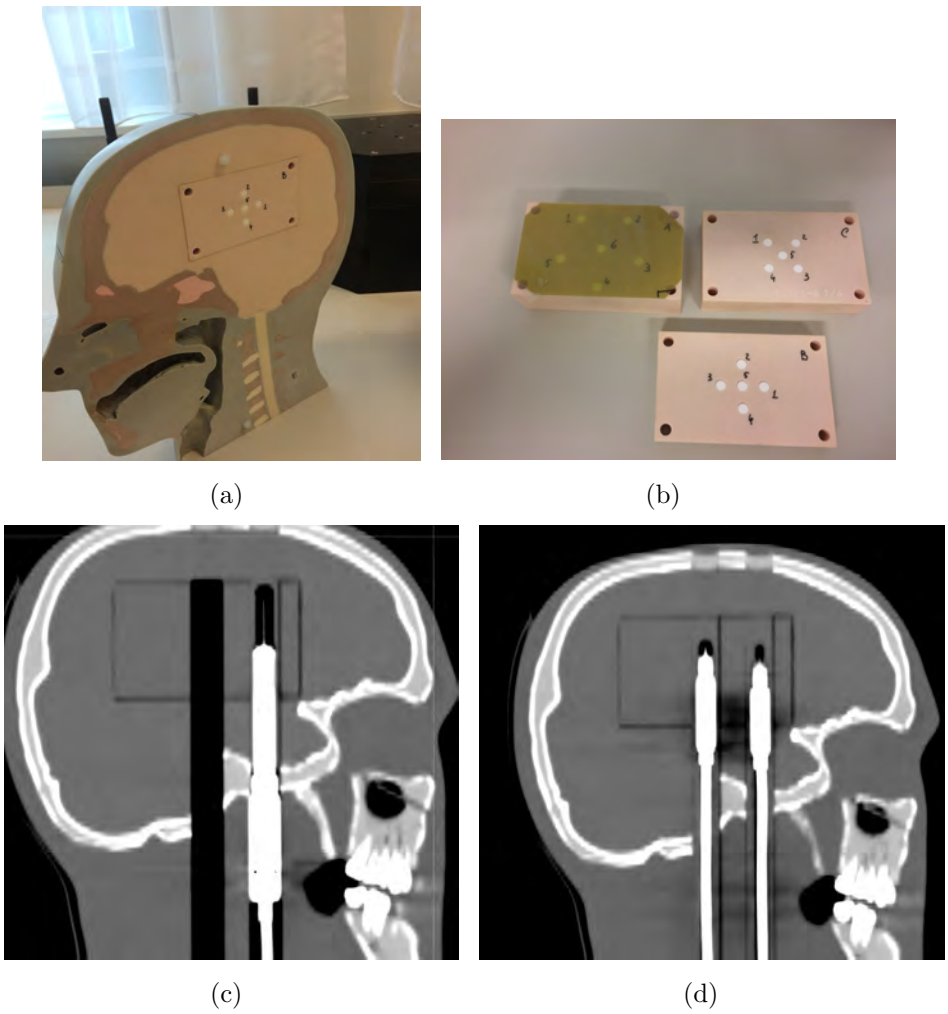

Figure 1. (a) Half bulk part of the head with alanine pellets inside. (b) Alanine pellets placed inside the cubic brain tissue equivalent insert. Each cubic insert is subdivided into three slices. (c) CT scan of the head with one Farmer chamber placed in the brain cavity. The second cavity is not filled in this image but during measurements it was filled either with a second chamber or substitute material. (d) CT scan of the head with a Semiflex and a Pinpoint chamber in the brain cavity.

A head phantom already used at the PSI facility (Albertini *et al* 2011) was customized in collaboration with CIRS (Tissue Simulation and Phantom Technology, Norfolk, Virginia USA). The head phantom is designed to be as close as possible to the real patient head geometry reproducing different tissue heterogeneities. It allows to verify the correct dose delivery for complex geometries due to the shape of entrance surface and irregular internal structures such as bone. This phantom has the advantage (compared to the common Alderson phantom) to be cut in the sagittal direction and thus avoiding air gaps between the plates along the beam axis' direction through which light ions could 'tunnel'. The phantom is sectioned in 20 mm increments for three EBT film locations in the cranio-caudal direction starting from the approximate center of the sagittal plane. The main advantage of this sectioning for film placement is the possibility to evaluate the effect of heterogeneities in the head-neck region on the dose distribution. The disadvantage is that the commercial version of the phantom was limited to film dosimetry only. To overcome this disadvantage and allow absolute dosimetry with ion chambers and alanine detectors, the head phantom has been customized by CIRS following MedAustron specifications. In particular, in the half bulk part of the head a rectangular brain cavity for placement of interchangeable dosimetry inserts has been created. Cubic brain tissue equivalent inserts of the size $5 \times 5 \times 8$ cm^3 were customized to allow measurements with alanine pellets and different ionization chambers (two Farmer TM30013, two Semiflex 0.125 cm^3 TM31010 and two PinPoint 0.03 cm^3 TM31015), as shown in figure 1.

The cubic brain insert for alanine pellets was subdivided in three slices and can allocate up to 22 alanine pellets for a single plan irradiation (see figure 1(b)). The pattern of the detector placement was customized in order to have a good coverage of the target volume and minimize the shadowing of the detectors in the Beam's eye view. All ionization chambers have a customized brain tissue equivalent sleeve to ensure that the effective point of measurements is at the center of the cubic brain insert in superior-inferior direction.

The CIRS dynamic pelvis phantom was designed for end-to-end testing including image acquisition, planning and dose delivery in image-guided radiation therapy. In the phantom there is the possibility to allocate

different water-equivalent interchangeable 6.35 cm cubes. The cubes accommodate ionization chambers, films or alanine pellets. The film stack cubic insert accommodates 13 radiochromic films with 4 mm spacing. The ionizations chamber cubes are designed for target acquisition and quantitative dose measurements. Each cube includes a target mimicking a 50 cm^3 prostate gland and is machined to receive the chamber at the center of the prostate volume. In particular, a Farmer TM30013, a Semiflex 0.125 cm^3 TM31010 and a PinPoint 0.03 cm^3 TM31015 can be placed inside the phantom. For the alanine pellet measurements water-equivalent cubic inserts have been sliced in three parts and can allocate up to 22 alanine pellets for a single plan irradiation. All of the above mentioned plastic materials composing the phantoms are tissue-equivalent only for photon beams. According to the authors knowledge there is no data in literature on their tissue-equivalence in proton beams. In this work the absorbed dose to water determined with a Farmer ionization chamber in the homogeneous and head phantom is reported and compared with alanine dosimetry. Measurements with the Farmer chamber could not be performed in the pelvis phantom due to a manufacturing deficiency. Other types of ionization chambers were not used.

2.2. Alanine electron paramagnetic resonance (EPR) dosimetry

The alanine EPR dosimetry was used as an independent method since the monitor chambers of the beam delivery system and the beam model of the TPS were both calibrated against ionization chamber dosimetry. The alanine detectors in form of pellets were provided by the National Physical Laboratory (NPL). The detectors have a nominal diameter of 5.0 mm and a thickness of about 2.3 mm. The NPL alanine detectors consist of 90.9% by weight L-α-alanine and 9.1% high melting point paraffin wax. On average the weight of the pellets used in the experiments at MedAustron was 55.1 mg with a standard deviation of 0.9 mg. The average density is around 1.22 g cm^{-3} actually close to PMMA (density 1.19 g cm^{-3}), but varies slightly from batch to batch. Thus in PMMA phantoms the perturbation effects were regarded negligible. In water equivalent phantoms, like the phantoms used in this work, the perturbations will be larger but it is expected to remain negligible in uniform dose regions. The pellets were handled with care; they are reasonably solid due to 10% of paraffin binder but still they can break or be crushed quite easily. The temperature during irradiation influences the response.

NPL supplied both irradiated and non-irradiated control dosimeters, which were stored and transported with the other pellets at all times (except during exposure). The dosimeters were conditioned at 55% relative humidity for ten weeks prior to use in order to reduce post-irradiation fading. After each irradiation the pellets were shipped to NPL in batches of 40 pellets, where they were evaluated following the standard procedure (Sharpe and Sephton 2000). Unlike ionization chambers, the dose response of solid state detectors like films or alanine depends explicitly on the charge, the fluence and the energy E of the particles which constitute the mixed radiation field. The sensitivity of a detector towards a given radiation quality can be expressed by its *relative effectiveness* (RE, symbol η) (Geiss *et al* 1998, Spielberger *et al* 2002, Herrmann 2012). The RE can be defined as:

$$\eta(Z,E) = \frac{D_{\mathrm{aln},^{60}\mathrm{Co}}}{D_{\mathrm{aln,\,p}}}\Big|_{\mathrm{iso-response}} \tag{1}$$

the ratio of the absorbed dose to alanine at low-LET radiation $D_{\mathrm{aln},^{60}\mathrm{Co}}$ (^{60}Co reference radiation) and the absorbed dose to alanine at the proton beam quality $D_{\mathrm{aln,\,p}}$, which yields the same detector response. This physical quantity is defined similarly as RBE for biological systems. In case that track overlapping effects on a microscopic level can be neglected, the relative effectiveness $\overline{\eta}_{\mathrm{aln}}$ for the field can be calculated from the binned energy spectra of all ions in the radiation field as a dose weighted average of the relative effectiveness (Katz 1993, Bassler *et al* 2008), $\eta_{\mathrm{aln}}(E_j, Z_i)$, of each ion type:

$$\overline{\eta}_{\mathrm{aln}} = \frac{\sum_{i=1}^{n_{\mathrm{proj}}}\sum_{j=1}^{n_{\mathrm{bin}}}\phi\left(E_j,Z_i\right)\times\left(\frac{S_{\mathrm{col}}}{\rho}\right)_{\mathrm{aln}}\left(E_j,Z_i\right)\times\eta_{\mathrm{aln}}\left(E_j,Z_i\right)}{\sum_{i=1}^{n_{\mathrm{proj}}}\sum_{j=1}^{n_{\mathrm{bin}}}\phi\left(E_j,Z_i\right)\times\left(\frac{S_{\mathrm{col}}}{\rho}\right)_{\mathrm{aln}}\left(E_j,Z_i\right)} \tag{2}$$

where the $\eta_{\mathrm{aln}}\left(E_j,Z_i\right)$ is the relative effectiveness of the particle Z_i with the energy E_j, $\phi\left(E_j,Z_i\right)$ is the fluence, $\left(\frac{S_{\mathrm{col}}}{\rho}\right)_{\mathrm{aln}}\left(E_j,Z_i\right)$ is the mass collision stopping power in pure alanine and the denominator of the equation is the total dose deposited in the volume of interest. In collaboration with RaySearch Laboratories AB (Stockholm, Sweden) we added a method for evaluating the correction for the 'quenching' of alanine pellets directly into the MC dose engine available in a research version of the RayStation TPS. In the MC code this was implemented by scoring the necessary quantities on the fly during a dose calculation. For proton energies above about 20 MeV the nominator and denominator of equation (2) were evaluated and accumulated at the mid point kinetic energy at voxel traversals. Below 20 MeV a special track-end stepper procedure is employed where the energy loss is divided into 90 logarithmic energy loss steps down to 20 keV kinetic energy. The same accumulation was performed at

each energy loss step. Finally, a contribution obtained by integrating numerically from 20 keV down to 1 keV is accumulated. It should be noted that the track-end procedure described above also accounts for possible voxel boundary crossings. The current version only considers protons (primary and secondary). A future version will also consider other secondaries like deuterons and alphas.

ICRU report 49 (International Commission on Radiation Units and Measurements 1993) presents the most comprehensive set of stopping power data available in literature. However, no stopping power data for pure alanine and alanine pellet composition are reported. In previous work (Onori *et al* 1997) calculated stopping powers for alanine by applying Bragg's rule to the stopping powers of the elementary constituents. However, this rule does not account for the influence of chemical binding effects. Based on the report published by NPL in 2006 (Palmans *et al* 2006) the mass collision stopping power in pure alanine and in the alanine pellet material (90.9% by weight L-α-alanine and 9.1% paraffin wax) were computed. Stopping powers for each element were taken from ICRU 49. Large deviations (up to 3.4%) between the stopping power in pure alanine and in alanine pellets were found for energies below 0.1 MeV. Those data were implemented in the MC code of RayStation. In particular both stopping powers were used in the simulation:

- since the ranges of produced electrons are smaller than the alanine grain dimensions (from 5 to 200 μm), all electrons contribute to the total dose originated in the alanine grains. Therefore, to compute the dose weighted RE as reported in equation (2) we used the mass collision stopping power for pure alanine;
- for macroscopic transport in the MC code every step (on average) takes the proton through a mix of the alanine and paraffin binder and thus to calculate the mean energy loss the mass stopping power of the mixture (alanine pellet) needs to be considered.

RE a look-up table for protons based on the Hansen-Olsen model (Hansen and Olsen 1985) lately reviewed by Herrmann (2012) was hardcoded in the MC code. Different stopping power values were used in the calculation of the RE for protons as reported in Herrmann (2012) but this is assumed to have a negligible impact. The contribution of particles heavier than protons (e.g. deuterium and alpha particles) was neglected. For each beam alanine dose weighted average RE $\overline{\eta}_{\mathrm{aln}}$ was scored in each voxel of the whole dose grid (3D $\overline{\eta}_{\mathrm{aln}}$ distribution), as shown in figure 2. Based on the CT images of the phantoms the alanine pellets were contoured as cylinders of 5 mm diameter and 2.3 mm length. The calculation of 3D RE corrections was performed in a dose grid of $1 \times 1 \times 1\,\mathrm{mm}^3$ and an average value of $\langle \overline{\eta}_{\mathrm{aln}} \rangle_{\mathrm{pellet}}$ was extracted at each pellet position. In case the plan consisted of more than one beam, the RE at each pellet position was weighted by the dose contribution to the pellet given by each beam as reported in equation (3).

$$\langle \overline{\eta}_{\mathrm{aln}} \rangle_{\mathrm{pellet,\ plan}} = \frac{\sum_{i=1}^{n} \langle \overline{\eta}_{\mathrm{aln}} \rangle_{\mathrm{pellet},i} \times D_{w,i}}{\sum_{i=1}^{n} D_{w,i}} \tag{3}$$

where n is the number of beams in the plan, $\langle \overline{\eta}_{\mathrm{aln}} \rangle_{\mathrm{pellet},i}$ is the average of RE contributions to the pellet computed for the ith beam and $D_{w,i}$ is the dose to water contribution to the pellet for the ith beam. Strictly, the weighting should be done with dose to alanine values but these values are not available from the TPS and considering the almost constancy of the stopping power ratio alanine to water as a function of proton energy this is assumed to have negligible influence. The relative effectiveness derived from MC calculations is given in terms of absorbed dose to alanine but for comparison with the TPS a conversion into absorbed dose to water had to be performed. In the following the dose is denoted by D_{aln} and D_w to distinguish between absorbed dose to alanine and to water. Then equation (1) can be reformulated to:

$$D_{\mathrm{aln,\,p}} = \frac{D_{\mathrm{aln},^{60}\mathrm{Co}}}{\langle \overline{\eta}_{\mathrm{aln}} \rangle_{\mathrm{pellet,\ plan}}} \tag{4}$$

where $D_{\mathrm{aln},^{60}\mathrm{Co}}$ is the absorbed dose to alanine in ^{60}Co, $D_{\mathrm{aln,\,p}}$ is a the absorbed dose to alanine in proton beam and $\langle \overline{\eta}_{\mathrm{aln}} \rangle_{\mathrm{pellet,\ plan}}$ is the RE computed at each pellet position for a generic composite treatment plan. In order to convert dose to alanine in dose to water the mass stopping power ratio water to alanine $\left(\frac{s_{\mathrm{col}}^{p}}{\rho}\right)_{\mathrm{aln}}^{w}$ for the proton beam has to be computed. The value $\left(\frac{s_{\mathrm{col}}^{p}}{\rho}\right)_{\mathrm{aln}}^{w} = 1.024$ was derived via Monte Carlo simulation as reported in Ableitinger *et al* (2013) based on stopping power values from tables in ICRU report 73 (International Commission on Radiation Units and Measurements 2005) and ICRU report 49 (International Commission on Radiation Units and Measurements 1993). Then following the approach used in Ableitinger *et al* (2013) the proton absorbed dose to water derived from alanine (pDw) can be written as:

$$D_{w,p} \approx \frac{D_{w,^{60}\mathrm{Co}}}{\langle \overline{\eta}_{\mathrm{aln}} \rangle_{\mathrm{pellet,plan}}} \times \left(\frac{s_{\mathrm{col}}^{p}}{\rho}\right)_{\mathrm{aln}}^{w} \times \left(\frac{\mu_{\mathrm{en}}^{^{60}\mathrm{Co}}}{\rho}\right)_{w}^{\mathrm{aln}} \tag{5}$$

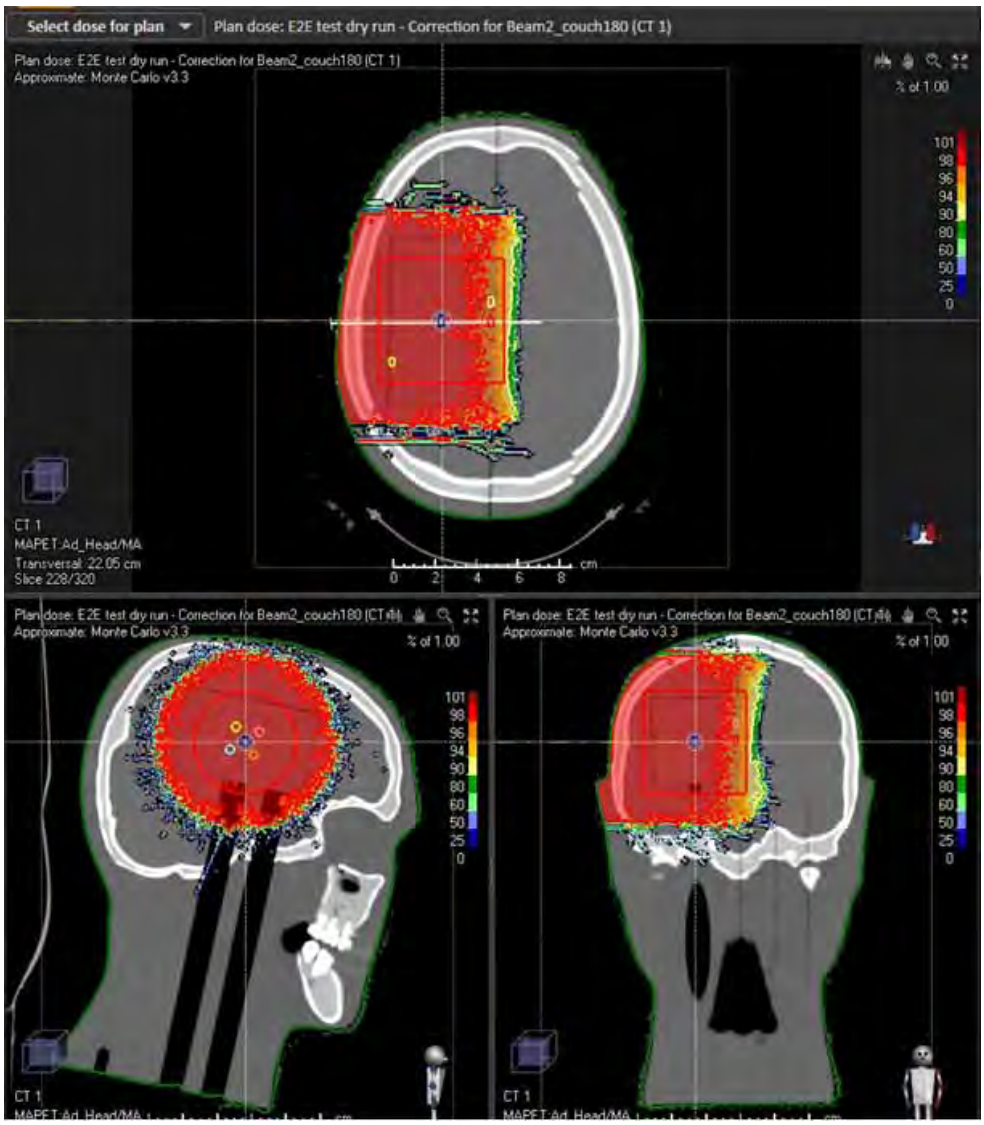

Figure 2. 3D $\overline{\eta}_{aln}$ distribution for one lateral beam in the head phantom. Transversal, coronal and sagittal views of the head phantom in the evaluation version of RayStation.

where $D_{w,^{60}Co}$ is the Co-60 equivalent absorbed dose to water derived from alanine (*CoEQDw*) as provided by NPL and $\left(\frac{\mu_{en}^{^{60}Co}}{\rho}\right)_w^{aln}$ is the ratio of mass energy absorption coefficients of water and the pellet us alanine/paraffin wax mixture for ^{60}Co. Regarding $\left(\frac{\mu_{en}^{^{60}Co}}{\rho}\right)_w^{aln}$ a constant value 0.976 was recommended by NPL. The approximation sign in equation (5) refers to the fact that no exact or more sophisticated cavity theory for the Co-60 calibration beam is used and because we neglect any fluence perturbation correction factors (Ableitinger *et al* 2013). An analysis of the uncertainties related to all involved parameters is reported in section 3.2.1.

2.3. Ionization chambers

As mentioned above, all the phantoms were designed in such a way that different ionization chamber inserts can be placed perpendicular to the beam direction. This enabled the use of ionization chambers calibrated in terms of absorbed dose to water which are the most commonly recommended reference dosimeters for clinical dosimetry. In this study an assembly of a PTW Unidos Webline electrometer and a PTW Farmer chamber (Type TM30013) was used. In order to avoid signal saturation due to the high dose rate the range of the electrometer was set to medium. An operating voltage of +400 V was applied. Correction factors for recombination and polarity effects were assumed to be unity, since measurements carried out in our proton beam (synchrotron-based) showed a negligible contribution of those two effects on the Farmer chambers. The chambers were calibrated in terms of absorbed dose to water N_{D,w,Q_0} in ^{60}Co at the Secondary Standard Dosimetry Laboratory (SSDL) of Seibersdorf Laboratories (Austria). The $k_{Q_p,Q_0} = 1.030 \pm 0.018$ was the beam quality correction factor derived from TRS 398 (International Atomic Energy Agency 2000) as the average value over the range of beam qualities encountered in the end-to-end tests.

2.4. EBT3 radiochromic films

In order to check the homogeneity of 2D dose distributions the plastic phantoms were loaded with GafChromic EBT3 films in addition to the alanine pellets. These films are sensitive for doses up to 10 Gy (Martišíková *et al* 2008, Martišíková and Jäkel 2010). As all the solid state detectors also EBT3 films are subject to 'quenching' effects (Martišíková *et al* 2008, Fiorini *et al* 2014). Thus, in order to use them for absolute measurements we would need to predict RE corrections based on a model (Spielberger *et al* 2002) as it was done for the alanine. In this work the focus was rather on an evaluation of their relative dose response. To characterize transverse dose profiles measured with films, the parametrization was taken from Gall *et al* (1993) as recommended by ICRU78 (International Commission on Radiation Units and Measurements 2007). The lateral field homogeneity (in percent) was defined as:

$$\mathrm{HI} = \frac{\mathrm{Max} - \mathrm{Min}}{\mathrm{Max} + \mathrm{Min}} \times 100 \tag{6}$$

where Max and Min are the maximum and minimum doses evaluated in the treatment width. Moreover, the lateral penumbra of a transverse profile is the distance between two dose points measured in the lateral fall-off between the 80% and 20% dose levels (LP_{80-20}). Treatment width was defined as the distance between two lateral penumbrae LP_{80-20} widths ($2 \times LP_{80-20}$) from the 50 percent isodose levels of the lateral-beam profile. For each plan films were irradiated in different depths and then scanned with Epson Expression 11000XL Pro in transmission mode after 24 h. The read-out procedure was based on Dreindl *et al* (2014).

2.5. End-to-end test procedures

During testing, the three phantoms were transferred through the workflow like real patients to simulate the entire clinical procedure. The first step was the registration of the test patients (phantoms) in the *oncology information system (OIS)* with demographics data (name, surname, gender, date of birth, etc). The three phantoms were prepared with dummy pellets made of the same tissue-equivalent materials of the inserts. The *head phantom* was immobilized with a thermo-plastic mask on the Base of Skull (BoS) extension plate from QFix for typical head and head&neck cases. The mask was left on the phantom for one night in order to minimize the shrinkage. The CT scans were acquired with pre-defined scan protocols used at MedAustron for cranial and pelvic treatments. The CT images were transferred from the CT console via the *picture archiving and communication system (PACS)* to the TPS RayStation v5.0.

Regarding the *homogeneous phantom* a target of $8 \times 8 \times 12$ cm^3 located symmetrically around the isocenter was outlined. Moreover, at the position of each alanine pellet a Region of Interest (ROI) was drawn. A physical dose of 10 Gy was planned to the target volume in order to achieve a readout reproducibility better than 0.5% on the dose delivered to the alanine pellets. This configuration and planned target volume reproduced those from the paper by Ableitinger *et al* (2013) in order to benchmark our data. Measurements were carried out in two measurement sessions over one month. In order to be consistent, corrections for the relative effectiveness (RE) were applied to the measurements as reported in the paper (Ableitinger *et al* 2013) and based on FLUKA MC simulations.

Concerning the *Head phantom*, three different clinical scenarios of increasing complexity were simulated.

(i) The first scenario was a configuration with a single beam (Gantry 90°, couch 0°) in isocentric condition (isocenter at the center of the target volume and large air gap of 60 cm). A cylindrical target of 7 cm in diameter and 6.5 cm in height (250 cm^3) was delineated on the CT scans in order to homogeneously cover all the pellets. A physical dose of 10 Gy was planned to the target volume (see figure 3(a)).

(ii) The second scenario was a configuration with two oblique beams (both beams at Gantry 90°, with the couch tilted to 350° and 190°). In order to be closer to a real patient treatment scenario at MedAustron, the irradiation was performed in non-isocentric condition for both beams. Therefore, the head phantom was moved towards the nozzle in order to minimize the air gap (15 cm). A physical dose of 10 Gy was planned to the target volume (see figure 3(b)). A weight of 104 kg was placed on the table top to simulate the real patient weight.

(iii) The third scenario was very similar to the second one. The main difference was that one of the two beams needed a range shifter as the target volume was extended to the phantom surface (see figure 3(c)).

Regarding the *Pelvis phantom*, as for the *Head phantom*, a cylindrical target of 7 cm in diameter and 6.5 cm in height (250 cm^3) was delineated on the CT scans. Two treatment plans were created: one plan consisted of a 'single beam' (Gantry 90°, couch 0°) and the other plan consists of two 'opposing beams' (Gantry 90°, couch 0° and 180°). A physical dose of 10 Gy was planned to the target volume for both treatment plans.

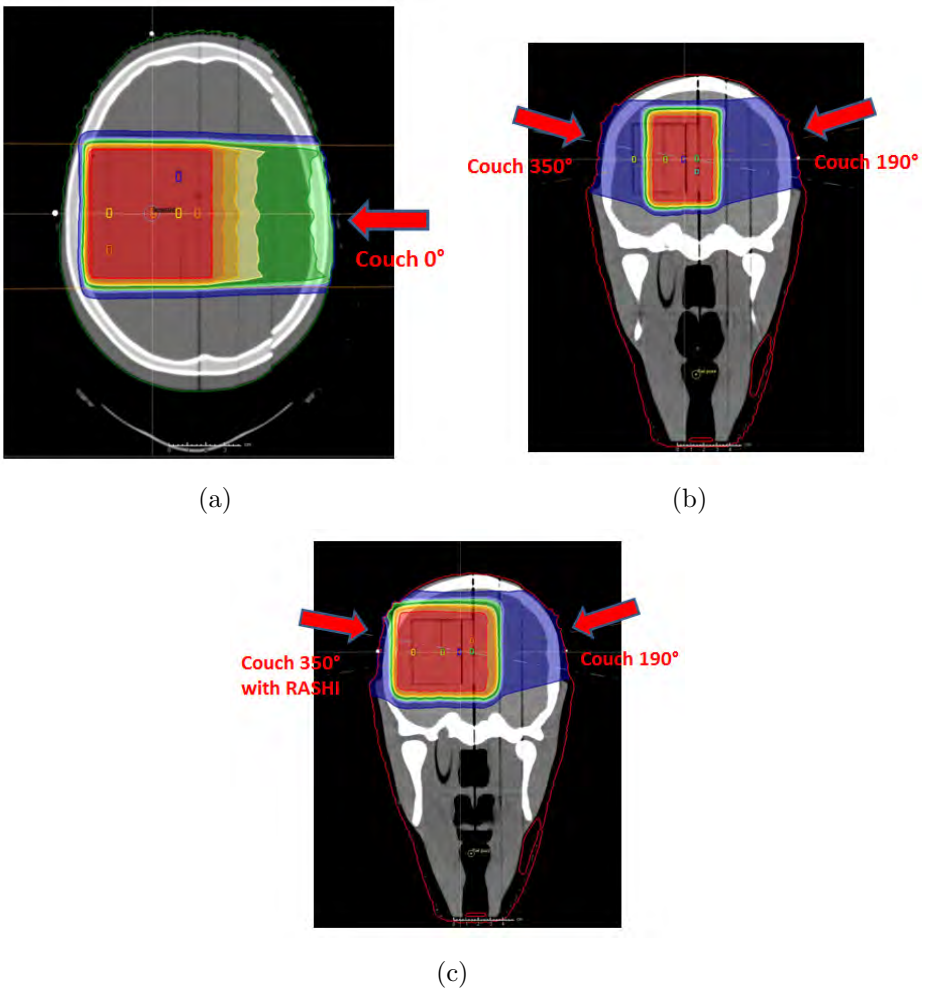

Figure 3. Dose distributions for the three clinical scenarios in the *Head phantom*. The red arrows represents the beams' directions. The first scenario with one beam in (a), in (b) the second scenario with two oblique beams and in (c) the third scenario with two oblique beams and range shifter.

All the treatment plans were exported to the *OIS* and irradiated at the horizontal beam line (HBL) of irradiation room 3 at MedAustron. The *homogeneous phantom* was loaded with 20 alanine pellets and two EBT films for the first irradiation and with Farmer chamber (TM30013) and dummy pellets for the second irradiation. The *homogeneous phantom* was aligned with in-room lasers for both irradiations.

The *Head phantom* was loaded with 22 alanine pellets and two EBT films for the first irradiation and with two Farmer chambers (TM30013) for the second irradiation. The *Head phantom* on the BoS frame was positioned on the robotic couch in IR3. Two x-rays images (one A-P projection and one lateral projection) were acquired with the innovative ring imaging system (medPhoton GmbH, Salzburg, Austria) (Zechner *et al* 2016). A 2D/3D image registration with on-the-fly digitally reconstructed radiographs (DRRs) reconstructed from the CT scan was performed. A setup correction vector based on 2D/3D image registration was applied. The robotic couch moved to the treatment position including the correction vector (see figure 4). A light based tracking camera installed on the floor corrects on-line for setup errors and the bending of the couch in comparison to the planning CT.

The *Pelvis phantom* was loaded with 22 alanine pellets and two EBT films. The in-room workflow was performed in a similar way as for the head phantom.

2.6. Comparison of alanine dosimetry with ionization chamber dosimetry in water

IAEA TRS 398 (International Atomic Energy Agency 2000) recommends water as the reference medium for the determination of absorbed dose with proton beams and the work by Lourenço *et al* (2017) shows that difference in fluence between plastic substitutes and water can differ by 1–2%. To investigate if this effect would contribute to the 2% difference between alanine and ionization chamber dosimetry, a comparison in water was performed. The measurements were carried out in a stationary water phantom MP1 (PTW, Freiburg) with a 3 mm thin PMMA entrance window. The only movable axis of the MP1 water phantom is in depth with 0.1 mm resolution. The phantom was set up with the outer surface of the thin window at the isocenter. Since alanine pellets are hygroscopic they need to be waterproofed before inserting them into the water phantom. Customized holders

Figure 4. The experimental setup of the *Head phantom* fixed with the thermo-plastic mask on the BoS frame and loaded with alanine pellets and EBT films. A patient-equivalent weight of 104 kg was placed on the table top and the light based tracking camera including feedback loop to the robotic positioning system corrected for setup errors and the bending of the couch in comparison to the planning CT.

were provided together with the alanine pellets by NPL. The holders (F-type) had the same outer dimensions (7 mm diameter) as the Farmer chamber and can be placed inside the same plastic sleeve commercially designed for the Farmer. In each F-type holder nine alanine pellets were positioned. An additional plastic rod of 15 cm can be screwed on the F-type holder to insert and remove it easily from the plastic Farmer sleeve. The same commercial Farmer sleeve was used for accurately positioning the stack of nine alanine pellets and the Farmer ionization chamber (TM30013) at the same measurement depths in water. Two different plans were irradiated:

(i) a single-layer scanned field 7×7 cm^2 of energy 179.2 MeV. Measurements were carried out at the clinical reference depth z_{ref} of 20 mm in water. Both detectors were irradiated with a physical dose of 10 Gy;
(ii) a fully modulated scanned field of $6 \times 6 \times 6$ cm^3 with the center of SOBP positioned at the water equivalent depth (WED) of 15 cm. Measurements were carried out at two different residual range: $R_{res} = 2$ cm and $R_{res} = 4$ cm. A physical dose of 10 Gy was delivered to the target volume.

However, the effective point of measurement is different for alanine and the Farmer chamber:

- for the Farmer chamber the reference point, located on the central axis at the centre of the cavity volume, was positioned at a distance $0.75 \times r_{cyl} = 2.3$ mm (International Atomic Energy Agency 2000, Palmans and Vatnitsky 2016) away from the source (i.e. deeper in water).
- for the alanine pellet the reference point, corresponding to the center of mass of the detector, was positioned at the reference depth z_{ref}. The alanine pellet material has a mass density very close to that of water (1.22 g cm^{-3} on average) and therefore the effective point of measurement is shifted by not more than 0.2 mm from the center of mass. Given the low gradient at the measurement point in the calibration energy this has a negligible correction and we have not applied a displacement correction for the alanine pellet.

3. Results

3.1. Measurements in plastic phantoms

Figure 5 shows the comparison among the planned absorbed dose determined with the TPS (PB algorithm), the *CoEQDw* and the *pDw* using equation (5) for the homogeneous phantom. The error bars in this graph as well as any subsequent graphs and tables in the paper represent standard deviations.

In figure 6 the planned absorbed dose determined with the TPS (PB algorithm), the *CoEQDw* and the *pDw* using equation (5) are shown as function of the R_{res} for the homogenous phantom. As expected the RE corrections were bigger (up to 3.5%) for larger depths close to the distal part of the SOBP ($R_{res} = 2.0$ cm pellets from number 1 to 5 in figure 7).

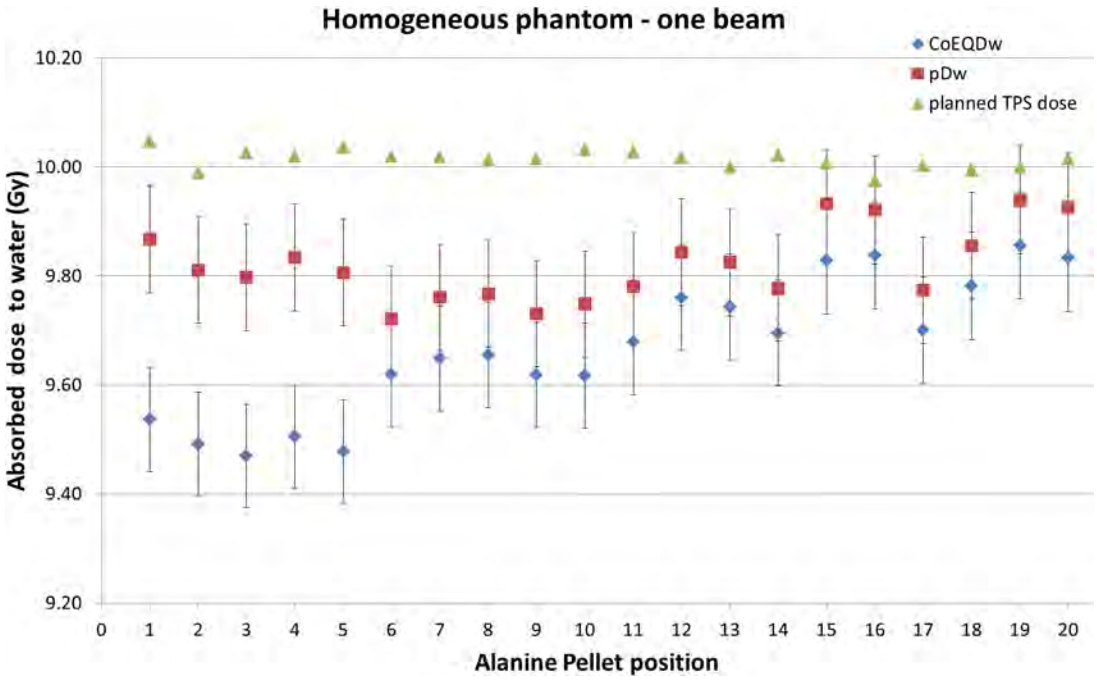

Figure 5. Comparison of TPS planned dose, the *CoEQDw* and the *pDw* determined with equation (5). RE corrections derived from Ableitinger *et al* (2013).

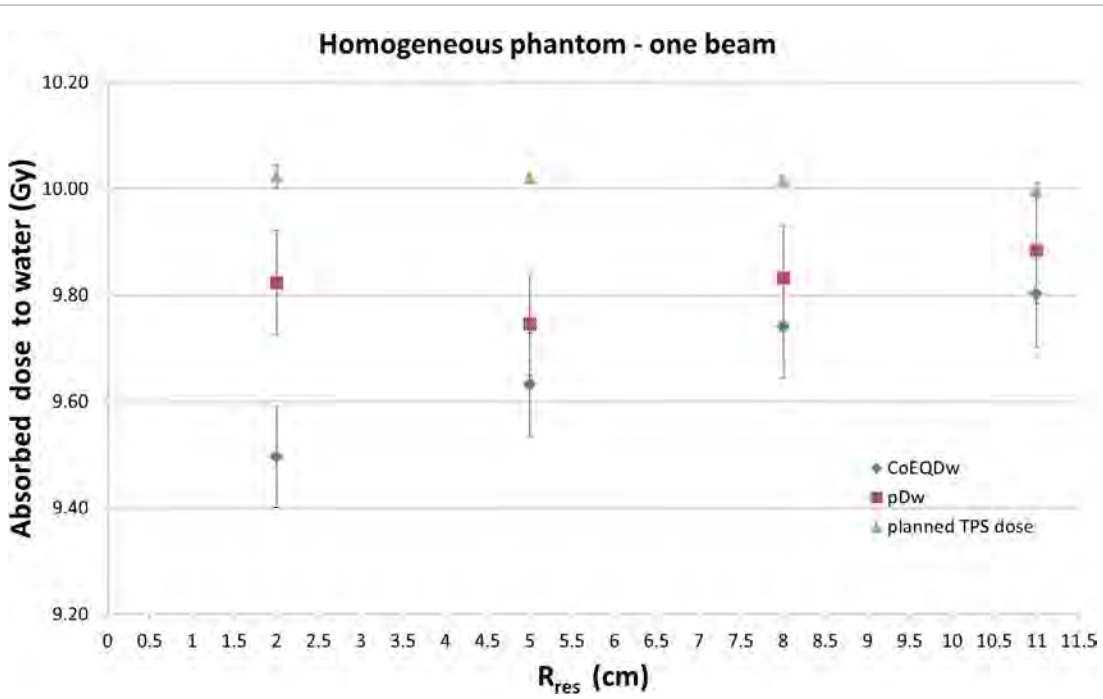

Figure 6. TPS planned dose, the *CoEQDw* and the *pDw* determined with equation (5) as function of the R_{res} for the homogenous phantom. Each point of the plot is the average of 5 alanine pellets' readings at a certain depth in the phantom. RE corrections derived from Ableitinger *et al* (2013).

Figure 7 shows the deviation between *pDw* and TPS planned dose (PB algorithm) for the homogeneous phantom. As one can see in figure 7 the measurements over one month were very reproducible with all the pellets within one standard deviation. Table 1 shows the overall mean of deviations of alanine pellets from the TPS planned dose. The data in the table show a very good reproducibility of the measurements within 0.3% over one month. The measured dose by alanine pellets is on average 2% smaller than the planned dose after correction for quenching. Similar behavior was found and reported in the paper of Ableitinger *et al* (2013) with measurements carried out at HIT (Heidelberg, Germany). Regarding the measurements acquired with the Farmer chamber at the center of the target volume a very good reproducibility of the beam delivery was measured as for the alanine

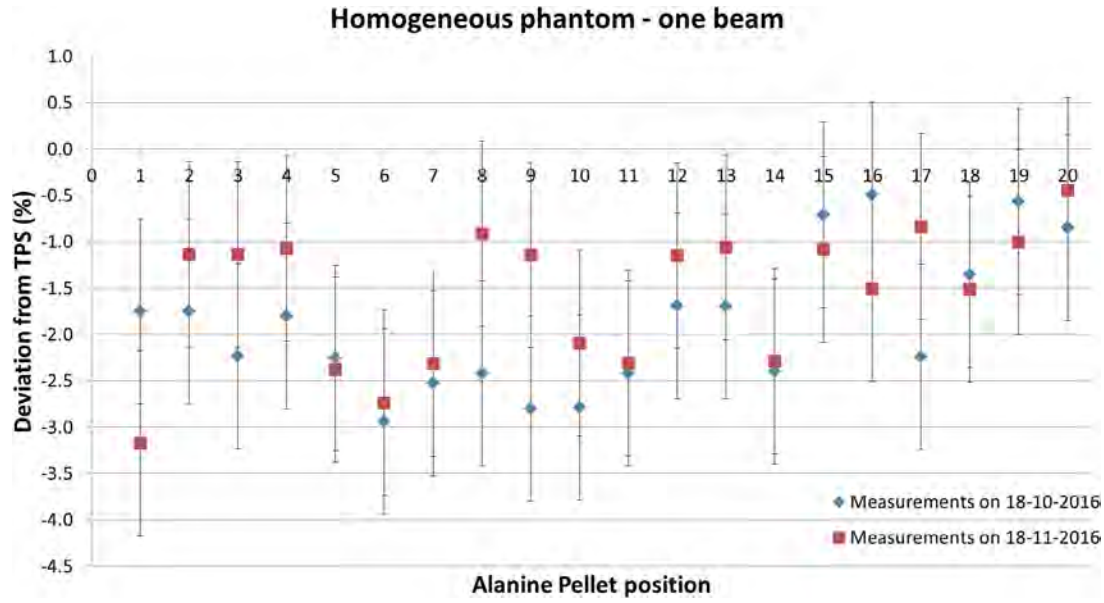

Figure 7. Deviations between *pDw* and TPS planned dose. RE corrections derived from Ableitinger *et al* (2013). In blue the data measured on 18 October 2016 and in red the data measured one month later.

Table 1. Overall mean deviations of *pDw* from TPS planned dose (PB algorithm) for the end-to-end test planned in the homogeneous phantom. RE corrections derived from Ableitinger *et al* (2013).

	Deviations alanine-TPS (PB) (%) (date 18 October 2016)	Deviations alanine-TPS (PB) (%) (date 18 November 2016)
Mean	−1.9	−1.6
Standard deviation	0.8	0.7
Minimum deviation	−0.5	−0.4
Maximum deviation	−2.9	−3.2

Table 2. Overall mean deviations of alanine pellets from Farmer chamber measurements for the end-to-end test planned in the homogeneous phantom. RE corrections derived from Ableitinger *et al* (2013).

	Deviations alanine-Farmer (%) (date 18 October 2016)	Deviations alanine-Farmer (%) (date 18 November 2016)
Mean	−2.9	−2.3
Standard deviation	0.7	0.7
Minimum deviation	−1.7	−1.1
Maximum deviation	−3.9	−3.6

pellets (within 0.3%). However, as one can see in table 2 the average dose obtained from the alanine pellets systematically deviated from dose derived with Farmer chamber up to 2.9%.

For each of the two EBT3 films different transverse dose profiles have been analyzed at 10 mm distance. The average homogeneity index HI was respectively 2.5 ± 0.3% and 2.3 ± 0.4% and hence within our 5% clinical tolerance level.

Concerning the measurements in the *Head phantom* in figure 8 we report the measurements with alanine pellets in the simplest clinical scenario with a single beam in isocentric condition (see figure 3(a)). Table 3 shows the overall mean of deviations of alanine pellets from the TPS planned dose and from the Farmer measurements. From figure 8 and table 3 the alanine pellets measurements were reproducible within 0.4% on average. Again a systematic underestimation of about 2% of the dose derived with alanine in comparison to the TPS planned dose was found. Moreover, a systematic deviation between the Farmer chamber measurement at the center of the volume with the alanine pellets was confirmed also in the *Head phantom*. For the irradiated EBT3 film the HI along the central cross-sectional profile in PA direction was 2.3% hence within our 5% clinical tolerance level. Measurements in a more complex clinical scenario with two oblique beams in non-isocentric condition (small air gap) were carried out as described in section 2.5 (see figure 3(b)). As it is shown in figure 9 the alanine pellets systematically underestimated the planned TPS dose by 2% as in the previous experiments. The pellets from

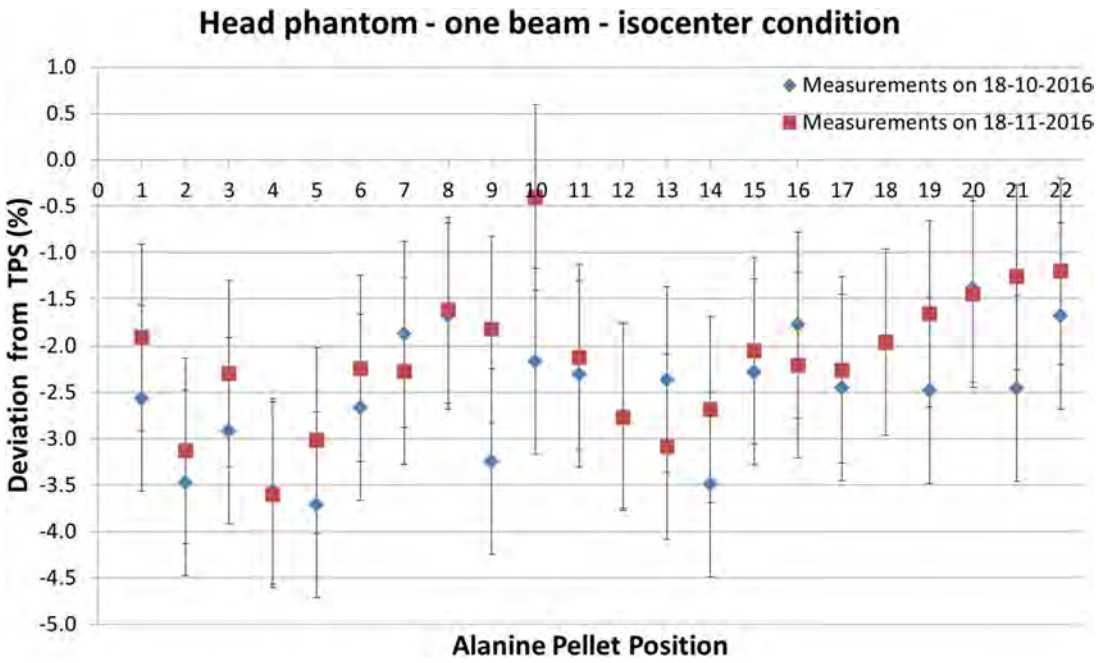

Figure 8. Deviations between *pDw* and TPS planned dose. The alanine readings are corrected for the RE as described in section 2.2. In blue the data measured on 18 October 2016 and in red the data measured one month later.

Table 3. Overall mean deviations of *pDw* from TPS planned dose and from the Farmer measurements for the single beam irradiation in the *head phantom*. RE corrections derived as described in section 2.2.

	Deviation alanine-TPS (PB) on 18 October 2016 (%)	Deviation alanine-Farmer on 18 October 2016 (%)	Deviation alanine-TPS (PB) on 18 November 2016 (%)	Deviation alanine-Farmer on 18 November 2016 (%)
Mean	−2.5	−3.6	−2.1	−3.2
St. dev.	0.7	0.6	0.7	0.7
Min. dev.	−1.4	−2.4	−0.4	−1.9
Max. dev.	−3.7	−4.9	−3.6	−4.4

position 1 to 6 were exposed to a dose level lower (4 Gy) than the suggested 10 Gy by NPL. However, as one can see in the plot, the deviations from the TPS planned doses are comparable to the pellets positioned in the target but clearly with a larger spread and a larger uncertainty (in table 6 the 'NPL readout' is 1.5% instead of 1%). For the irradiated EBT3 film the HI along the central cross-sectional profile in PA direction was 3% and hence within our 5% clinical tolerance level.

As last step in order of clinical case complexity we carried out measurements in the *Head phantom* with two oblique beams in non-isocentric condition (small air gap) and one of the two beams with range shifter (see figure 3 (c)). Based on data acquired during the commissioning of the TPS, the pencil beam (PB) algorithm of RayStation v5.0 has some limitations and deficiencies in the dose calculation in the presence of range shifter, large air gaps, inhomogeneities of the medium and oblique incidence. Therefore, we recalculated the plan with the Monte Carlo (MC) algorithm implemented in a research version of the TPS. Note that there is no concern to use the same MC algorithm to compute the dose and the RE corrections since by the use of equation (2) to calculate the RE it is clear that there is no correlation of RE with the computed dose. In table 4 the overall mean of the deviations from PB and MC are reported. As expected, due to the limitations of PB, the MC algorithm showed smaller deviations in comparison to PB. For the MC algorithm an average deviation of −2% was found like in the other experiments in the homogeneous and the head phantom. For the irradiated EBT3 film the HI along the central cross-sectional profile in PA direction was 2.6% and hence within our 5% clinical tolerance level. In comparison to the measurements in the *homogeneous* and in the *head phantom* larger deviations were found in the *pelvis phantom*. Therefore, the plans were recomputed with an MC algorithm as for the plan with range shifter in the *head phantom*. Table 5 reports the overall mean of the deviations from PB and MC for both plans. As shown in table 5 the plan computed with MC algorithm partly reduces the deviations.

For the *pelvis phantom* a larger underestimation of about 4% was found mainly due to the non-tissue equivalence of bone materials (femoral heads) placed on the beam axis direction. For the two EBT3 films the average homogeneity HI along the central cross-sectional profile in PA and SI directions was respectively 2.8% and 2.9%

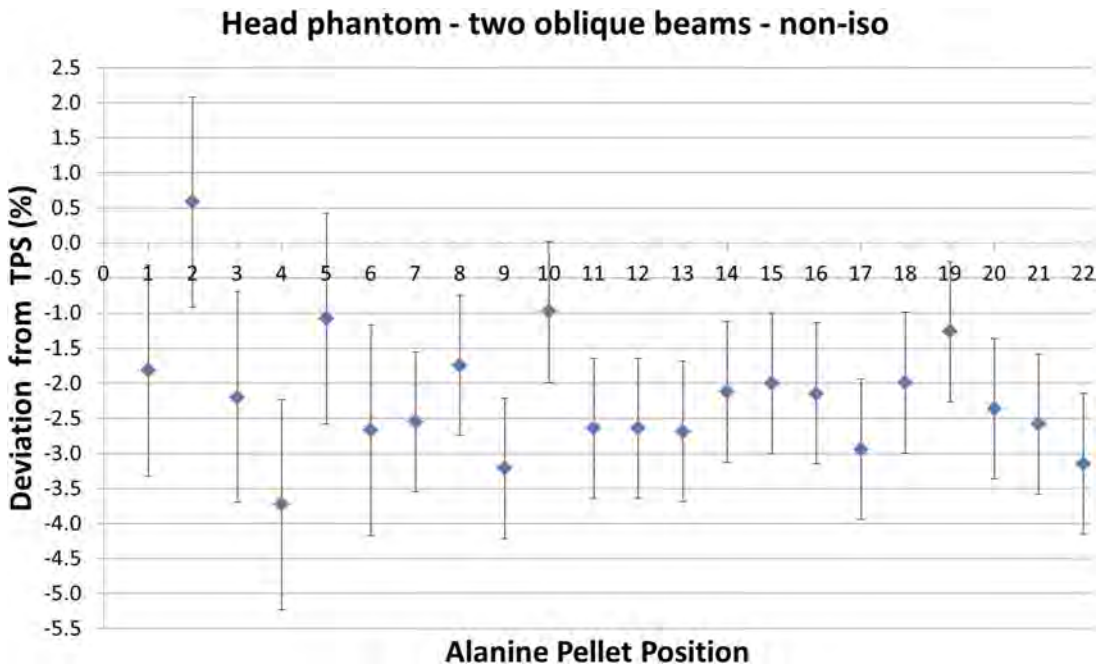

Figure 9. Deviations between *pDw* and the TPS planned dose. The data are corrected for the RE as described in section 2.2. Alanine pellets from 1 to 6 were irradiated with a dose of 4 Gy.

Table 4. Overall mean deviations of *pDw* from PB and MC algorithms implemented in RayStation TPS for the head phantom. RE corrections as described in section 2.2.

	Deviation alanine-TPS (PB) (%)	Deviation alanine-TPS (MC) (%)
Mean	−3.3	−2.0
Standard deviation	0.5	0.7
Minimum deviation	−2.6	−0.9
Maximum deviation	−4.2	−3.3

Table 5. Overall mean deviations of *pDw* from PB and MC algorithms implemented in RayStation TPS for the 'single beam' plan and the 'opposing beams' plan for the pelvis phantom. RE corrections were derived as described in section 2.2.

	Deviation alanine-PB 'single beam' (%)	Deviation alanine-PB 'opposing beams' (%)	Deviation alanine-MC 'single beam' (%)	Deviation alanine-MC 'opposing beams' (%)
Mean	−3.9	−4.0	−3.4	−3.5
St. dev.	1.4	1.1	1.4	0.7
Min. dev.	−1.0	−2.5	−0.3	−2.3
Max. dev.	−6.2	−6.0	−6.4	−5.0

for the 'single beam' plan and the 'opposing beams' plan. Both values are hence within our 5% clinical tolerance level.

3.2. Measurements in water phantom: alanine versus Farmer chamber

In order to minimize the 'quenching' effect of alanine pellets we carried out measurements in the plateau region ($z_{ref} = 20$ mm in water) in a single-layer scanned field 7×7 cm^2 of energy 179.2 MeV. At $z_{ref} = 20$ mm in water nine alanine pellets and the Farmer chamber (TM30013) were irradiated with a setup described in section 2.6. The alanine dose response was corrected as reported in section 2.2 with RE set to unity. The alanine pellets assess a lower absorbed dose to water in comparison to the Farmer chamber of $-2.5 \pm 0.3\%$ on average.

In addition, a comparison of alanine versus Farmer was performed in a fully modulated scanned field of $6 \times 6 \times 6$ cm^3 with the center of SOBP positioned at the WED of 15 cm. Average deviation of $-2.8 \pm 0.4\%$ was found at $R_{res} = 4$ cm and $-3.2 \pm 0.8\%$ was found at $R_{res} = 2$ cm. The quenching effect increased close to the distal part of the SOBP $R_{res} = 2$ cm as expected. The systematic deviation between the two dosimetric techniques (alanine EPR and ionization chamber) found on plastic phantoms was confirmed in water.

Table 6. Estimated relative standard uncertainty of $D_{w,p}$ when using equation (5). The combined uncertainty for the alanine pellet measurements are defined as the root mean square of the different components.

Physical quantity	Type A ($k = 1$) (%)	Type B ($k = 1$) (%)
NPL readout		1
RE corrections derived by MC	0.5	2
$(s^p/\rho)^w_{al}$		2
$(\mu^{Co}_{en}/\rho)^{al}_w$		0.5
Phantom setup		0.5
Combined standard uncertainty in $D_{w,p}$	3.0	

3.2.1. *Uncertainty budget*

All uncertainty estimates are made in accordance to the recommendations of the Guide to the expression of Uncertainty in Measurement (ISO/IEC 2008). The overall uncertainty on absorbed dose to water determined with thimble chambers in proton beams at MedAustron is 2% ($k = 1$) based on the guidance of the (International Atomic Energy Agency 2000). The uncertainties are dominated by the k_{Q,Q_0} contribution of 1.7%. In table 6 the estimated uncertainties of dose determination using alanine are reported. The combined uncertainty for the alanine pellet measurements were defined as the root mean square of the underlying initial components like NPL readout, MC simulation, stopping power ratio (uncertainty based on TRS-398), ratio of the mass energy absorption coefficients and phantoms setup. The uncertainty of the RE corrections derived by MC is dominated by the uncertainty of the Hansen and Olsen model itself. For the mass energy ratios for ^{60}Co the uncertainty is typically of the order of 0.5%. For the phantom setup 0.5% was estimated.

4. Discussion

Overall more than 230 alanine pellets were irradiated during end-to-end testing at MedAustron and all results are reported in this paper. No comparable set of data for consistency and reproducibility of results can be found in literature. Regarding the *homogenous phantom* the average deviations of alanine pellets with respect to the planned dose were $-1.9 \pm 0.8\%$ and $-1.6 \pm 0.7\%$. All the measured pellets were within 5% and very reproducible within 0.3% over one month. These results are in very good agreement (within one standard deviation) with the measurements carried out at HIT in which an average deviation of $-2.4 \pm 0.9\%$ was found for proton beams (Ableitinger *et al* 2013). The high reproducibility of the measurements and the excellent agreement with the results obtained at HIT was the basis for further investigations with more complex anthropomorphic phantoms.

For the 'single beam' plan in the *head phantom* (see figure 3(a)) measurements with alanine were very reproducible over one month with average deviations to the planned dose of $-2.5 \pm 0.7\%$ and $-2.1 \pm 0.7\%$. Deviations were slightly larger than the measurements in the *homogeneous phantom* but still within the uncertainty. Concerning the plan composed of two oblique beams in the *head phantom* (see figure 3(b)) average deviation of alanine in comparison to the planned dose was $-2.2 \pm 0.9\%$. Deviations were in agreement with the clinical case of one single beam and with the experiment performed in the *homogeneous phantom*. Moreover, for this specific indication, six alanine pellets were exposed to 4 Gy and still the deviations from the planned dose were comparable to the pellets exposed to 10 Gy. That is a very good indication for further applications of alanine pellet dosimetry at lower dose level closer to the prescription dose used for patient treatments (2–3 Gy/fraction). A more systematic investigation should be performed in order to apply alanine dosimetry at dose levels lower than 10 Gy. For the more complex clinical case with two oblique beams with range shifter (see figure 3(c)) the average deviation of alanine pellets to the PB algorithm were larger than the previous clinical cases ($-3.3 \pm 0.5\%$). However, the comparison with the plan recomputed with MC algorithm showed similar behavior as the other measurements with an average of $-2.0 \pm 0.7\%$.

In the *pelvis phantom* the deviations of alanine in comparison to the planned dose were larger than the measurements carried out in the homogeneous and head phantom. An average deviation of $-4.0 \pm 1.1\%$ was detected in the plan with two opposing beams. The recalculation with the MC algorithm in RS helped to reduce the difference down to $-3.5 \pm 0.7\%$ on average and -5.0% as maximum deviation. The larger deviations for the pelvis phantom may be due to the non-tissue equivalence of bone materials (femoral heads) placed on the beam axis direction. Indeed, the PB algorithm in the TPS considers the nuclear interaction in different materials compared to water. Therefore, the amount of high Z materials (e.g. ^{40}Ca in the bones) could result in a larger attenuation of primary proton fluence in the SOBP. This could be the reason why the measurements are much lower than the planned dose. The primary proton fluence attenuation is partly predicted by the MC algorithm but still the large uncertainties in the total cross-section data (up to 20% (ICRU 2000)) might explain the observed deviations. Further investigation on the fluence correction factors in different plastic materials needs to be carried out based on Monte Carlo simulations.

Table 7. The results of the comparison of alanine dosimetry and ionization chamber dosimetry. For each irradiation some information about the phantom and the characteristic of the irradiated field were reported. Moreover, mean and standard deviation of the overall deviations between doses determined either with alanine pellets or ionization chambers are shown.

Phantom type	Field	Mean (%)	Stdev (%)
Water phantom	Square field 7 × 7 cm^2 E 179.2 MeV	−2.5	0.3
Water phantom	Box 6 × 6 × 6 cm^3	−2.8	0.4
Water phantom	Box 6 × 6 × 6 cm^3	−3.2	0.8
Homogeneous phantom (18 October 2016)	Box 8 × 8 × 12 cm^3	−2.9	0.7
Homogeneous phantom (18 November 2016)	Box 8 × 8 × 12 cm^3	−2.3	0.7
Head phantom (18 October 2016)	Cylinder 250 cm^3	−3.6	0.6
Head phantom (18 November 2016)	Cylinder 250 cm^3	−3.2	0.7

For the measurements with EBT3 films only the relative dose response was considered. For each end-to-end test the plastic phantom was loaded with alanine pellets and EBT3 films in order to check the homogeneity of the 2D dose distribution. For all the films irradiated the homogeneity index HI (see equation (6)) was always better than 3% and hence within 5% clinical tolerance level established at MedAustron.

It was observed that, in all experiments carried out in plastic phantoms, alanine pellets assess a systematic lower dose than the Farmer ionization chamber. The systematic deviation between the two dosimetric techniques was around 2%. The monitor chamber of the beam delivery system and the beam model of the TPS were calibrated against ionization chamber dosimetry. Therefore, a 2% systematic deviation found between alanine and TPS planned dose can be attributed to the discrepancy between the two dosimetric techniques. Similar systematic deviation between alanine and Markus-type plane-parallel ionization chambers in PMMA was found by Fattibene *et al* (1996, 2002) and Onori *et al* (1996) in a 60 MeV proton beam. In higher energy proton beams similar underestimations were found by Ableitinger *et al* (2013) and Farr *et al* (2008) but not enough statistics were acquired in all those previous works in order to draw clear conclusions. An overview of the literature regarding the use of alanine as a dosimeter in clinical proton beams was presented by Palmans (2003).

More than 200 alanine pellets irradiated in this study show a consistent underestimation of alanine in comparison to ionization chambers in plastic phantoms. In this work, in addition to the measurements in plastic phantoms, a comparison of alanine versus Farmer chamber in water was performed. In table 7 the deviations between the absorbed dose to water determined with alanine pellets and ionization chambers are reported for each experiment in the scanned proton beams at MedAustron.

As one can see from table 7 a very consistent systematic mean deviation between the two dosimetric techniques was found for all experiments performed in different materials (water and plastic) and different irradiation fields. Considering the overall uncertainties of the two dosimetric techniques they agree within the uncertainty of measurement techniques (see section 3.2.1). This provides overwhelming and significant evidence that there exists one or more factors in the derivations of dose from alanine and/or from the ionization chambers that are responsible for the deviation. The systematic deviation is not yet understood and it could be related to the uncertainty on the k_{Q,Q_0} for the ionization chambers and RE, stopping power ratio water to alanine, perturbation factors for alanine pellets in proton beams or a combination of a number of these components. One source of uncertainty may be related to the beam quality correction factors k_{Q,Q_0} tabulated in TRS-398 for Farmer chamber (Gomà *et al* 2016). This is mainly an indication that perturbation factors in protons are not the assumed unity as in TRS-398 and they could be easily add up to 1% corrections. Stopping powers for alanine and alanine pellet mixtures have an uncertainty of up to 2%. Measurements of stopping power for the alanine pellet mixture were carried out in a proton beam at MedAustron. As a preliminary result we found a value for stopping power ratio water-to-alanine pellet material slightly higher (≈1.5%) than the calculated one. This could be an evidence that also the stopping ratio water-to-pure alanine could be slightly higher than the value 1.024 (Ableitinger *et al* 2013) used for our end-to-end tests. Further investigations based on Monte Carlo simulation would be beneficial. The Hansen-Olsen model (Hansen and Olsen 1985) used to derive RE corrections in proton beams presents several uncertainties mainly related to the selected radial dose distribution in the track structure model. Most of the data in literature validated the model for heavier ions than proton (Herrmann *et al* 2011, Herrmann 2012) (e.g. ^{12}C ions). The model may deviate substantially for protons as it is based on amorphous track structure models which may work better for the densely ionizing carbon ion track than for the more sparsely ionizing track of a proton. Further validation in a proton beam is necessary. Perturbation factors of alanine in proton beams are not known and might be an additional source of uncertainty. An estimation of those factors can be assessed by Monte Carlo simulation.

5. Conclusion

In conclusion, end-to-end tests are prerequisites for a clinical operation and they shall be performed as last step of medical commissioning of LIBT facilities. Since MedAustron started clinically with head and pelvis

treatments end-to-end tests described in this work were carried out in a proton beam for those two body sites. Based on the excellent results in terms of consistency and reproducibility of the end-to-end testing performed with different dosimetric techniques (alanine dosimetry, ionization chambers and EBT3 radiochromic films), it was demonstrated that the new scanned proton beam technology was safely integrated in clinical practice at MedAustron. A very consistent systematic deviation was found between the alanine dosimetry and the ionization chamber dosimetry in water and plastic materials. The investigation of the possible source of systematic uncertainties based on Monte Carlo simulations will be subject of future work at MedAustron. However, our experience showed that alanine pellets are suitable detectors for dosimetry audits in proton beam therapy and the developed procedures with customized anthropomorphic phantoms can be used to support implementation of scanning beam delivery technology in clinical practice.

Acknowledgments

We would like to thank the CIRS company for the customized design of head and pelvis anthropomorphic phantoms. The authors are grateful to Peter Sharpe (National Physical Laboratory) for fruitful discussions on the alanine EPR dosimetry.

References

Ableitinger A, Vatnitsky S, Herrmann R, Bassler N, Palmans H, Sharpe P, Ecker S, Chaudhri N, Jäkel O and Georg D 2013 Dosimetry auditing procedure with alanine dosimeters for light ion beam therapy *Radiother. Oncol.* **108** 99–106

Aguirre J, Alvarez P, Followill D, Ibbott G, Amador C and Tailor A 2009 Su-ff-t-306: optically stimulated light dosimetry: commissioning of an optically stimulated luminescence (OSL) system for remote dosimetry audits, the Radiological Physics Center experience *Med. Phys.* **36** 2591–2

Albertini F, Casiraghi M, Lorentini S, Rombi B and Lomax A 2011 Experimental verification of IMPT treatment plans in an anthropomorphic phantom in the presence of delivery uncertainties *Phys. Med. Biol.* **56** 4415

Bassler N *et al* 2008 The antiproton depth–dose curve measured with alanine detectors *Nucl. Instrum. Methods Phys. Res.* B **266** 929–36

Bäumer C, Ackermann B, Hillbrand M, Kaiser F J, Koska B, Latzel H, Lühr A, Menkel S and Timmermann B 2017 Dosimetry intercomparison of four proton therapy institutions in germany employing spot scanning *Z. Med. Phys.* **27** 80–5

Budgell G, Berresford J, Trainer M, Bradshaw E, Sharpe P and Williams P 2011 A national dosimetric audit of IMRT *Radiother. Oncol.* **99** 246–52

Clark C H *et al* 2009 Dosimetry audit for a multi-centre IMRT head and neck trial *Radiother. Oncol.* **93** 102–8

Clark C H *et al* 2014 A multi-institutional dosimetry audit of rotational intensity-modulated radiotherapy *Radiother. Oncol.* **113** 272–8

Dreindl R, Georg D and Stock M 2014 Radiochromic film dosimetry: considerations on precision and accuracy for EBT2 and EBT3 type films *Z. Med. Phys.* **24** 153–63

Eaton D J *et al* 2017 An external dosimetry audit programme to credential static and rotational IMRT delivery for clinical trials quality assurance *Phys. Med.* **35** 25–30

Farr J, Mascia A, Hsi W C, Allgower C, Jesseph F, Schreuder A, Wolanski M, Nichiporov D and Anferov V 2008 Clinical characterization of a proton beam continuous uniform scanning system with dose layer stacking *Med. Phys.* **35** 4945–54

Fattibene P, Calicchia A, d'Errico F, De Angelis C, Egger E and Onori S 1996 Preliminary assessment of LiF and alanine detectors for the dosimetry of proton therapy beams *Radiat. Prot. Dosim.* **66** 305–9

Fattibene P, De Angelis C, Onori S and Cherubini R 2002 Alanine response to proton beams in the 1.6–6.1 MeV energy range *Radiat. Prot. Dosim.* **101** 465–8

Fiorini F, Kirby D, Thompson J, Green S, Parker D, Jones B and Hill M 2014 Under-response correction for EBT3 films in the presence of proton spread out Bragg peaks *Phys. Med.* **30** 454–61

Fukumura A *et al* 1998 Carbon beam dosimetry intercomparison at HIMAC *Phys. Med. Biol.* **43** 3459

Gall K P *et al* 1993 State of the art? New proton medical facilities for the Massachusetts General Hospital and the University of California Davis Medical Center *Nucl. Instrum. Methods Phys. Res.* B **79** 881–4

Geiss O, Krämer M and Kraft G 1998 Efficiency of thermoluminescent detectors to heavy charged particles *Nucl. Instrum. Methods Phys. Res.* **142** 592–8

Gomà C, Andreo P and Sempau J 2016 Monte Carlo calculation of beam quality correction factors in proton beams using detailed simulation of ionization chambers *Phys. Med. Biol.* **61** 2389

Hansen J and Olsen K 1985 Theoretical and experimental radiation effectiveness of the free radical dosimeter alanine to irradiation with heavy charged particles *Radiat. Res.* **104** 15–27

Herrmann R 2012 Prediction of the response behaviour of one-hit detectors in particle beams *PhD Thesis* Aarhus University, Denmark

Herrmann R, Jäkel O, Palmans H, Sharpe P and Bassler N 2011 Dose response of alanine detectors irradiated with carbon ion beams *Med. Phys.* **38** 1859–66

IAEA 2000 Absorbed dose determination in external beam radiotherapy an international code of practice for dosimetry based on standards of absorbed dose to water *Technical Reports Series* 398, International Atomic Energy Agency, Vienna, Austria

Ibbott G S, Followill D S, Molineu H A, Lowenstein J R, Alvarez P E and Roll J E 2008 Challenges in credentialing institutions and participants in advanced technology multi-institutional clinical trials *Int. J. Radiat. Oncol. Biol. Phys.* **71** S71–5

ICRU 2000 Nuclear data for neutron and proton radiotherapy and for radiation protection dose *International Commission on Radiation Units and Measurements Report No.* 63 Bethesda, MA, US.

ICRU 1993 Stopping powers and ranges for protons and alpha particles *International Commission on Radiation Units and Measurements, Report No.* 49 Bethesda, MA, US

ICRU 2005 Stopping of ions heavier than helium *International Commission on Radiation Units and Measurements, Report No.* 73 Bethesda, MA, US

ICRU 2007 Prescribing, recording and reporting proton-beam therapy *International Commission on Radiation Units and Measurements,* Report No. 78 Bethesda, MA, US (https://doi.org/10.1016/j.ijrobp.2008.10.084)

ISO/IEC Guide 98-3 2008 *Uncertainty of Measurement—Part 3: Guide to the Expression of Uncertainty in Measurement* (International Organization for Standardization)

Katz R 1993 Relative effectiveness of mixed radiation fields *Radiat. Res.* **133** 390 (PMID: 8451392)

Kerns J R, Kry S F and Sahoo N 2012 Characteristics of optically stimulated luminescence dosimeters in the spread-out Bragg peak region of clinical proton beams *Med. Phys.* **39** 1854–63

Lourenço A *et al* 2017 Evaluation of the water-equivalence of plastic materials in low-and high-energy clinical proton beams *Phys. Med. Biol.* **62** 3883

Marrale M, Carlino A, Gallo S, Longo A, Panzeca S, Bolsi A, Hrbacek J and Lomax T 2016 EPR/alanine dosimetry for two therapeutic proton beams *Nucl. Instrum. Methods Phys. Res.* B **368** 96–102

Martišíková M, Ackermann B, Klemm S and Jäkel O 2008 Use of gafchromic® EBT films in heavy ion therapy *Nucl. Instrum. Methods Phys. Res.* A **591** 171–3

Martišíková M and Jäkel O 2010 Study of gafchromic® EBT film response over a large dose range *Phys. Med. Biol.* **55** N281

Moyers M, Ibbott G, Grant R, Summers P and Followill D 2014 Independent dose per monitor unit review of eight USA proton treatment facilities *Med. Phys.* **41** 012103

Onori S, d'Errico F, Angelis C D, Egger E, Fattibene P and Janovsky I 1997 Alanine dosimetry of proton therapy beams *Med. Phys.* **24** 447–53

Onori S *et al* 1996 Proton response of alanine based pellets and films *Appl. Radiat. Isot.* **47** 1201–4

Palmans H 2003 Effect of alanine energy response and phantom material on depth dose measurements in ocular proton beams *Technol. Cancer Res. Treat.* **2** 579–86

Palmans H and Vatnitsky S M 2016 Beam monitor calibration in scanned light-ion beams *Med. Phys.* **43** 5835–47

Palmans H, Thomas R, Shipley D and Kacperek A 2006 Light-ion beam dosimetry *NPL Report* DQL-RD 003 http://www.npl.co.uk/publications/light-ion-beam-dosimetry

Saini J, James S St, Traneus E, Wong T, Stewart R and Bloch C 2016 Su-f-t-155: validation of a commercial monte carlo dose calculation algorithm for proton therapy *Med. Phys.* **43** 3497

Schaeken B, Cuypers R, Lelie S, Schroeyers W, Schreurs S, Janssens H and Verellen D 2011 Implementation of alanine/EPR as transfer dosimetry system in a radiotherapy audit programme in Belgium *Radiother. Oncol.* **99** 94–6

Sharpe P and Sephton J 2000 An automated system for the measurement of alanine/EPR dosimeters *Appl. Radiat. Isot.* **52** 1185–8

Spielberger B, Scholz M, Krämer M and Kraft G 2002 Calculation of the x-ray film response to heavy charged particle irradiation *Phys. Med. Biol.* **47** 4107

Vatnitsky S *et al* 1999 Proton dosimetry intercomparison based on the ICRU report 59 protocol *Radiother. Oncol.* **51** 273–9

Zechner A, Stock M, Kellner D, Ziegler I, Keuschnigg P, Huber P, Mayer U, Sedlmayer F, Deutschmann H and Steininger P 2016 Development and first use of a novel cylindrical ball bearing phantom for 9-DOF geometric calibrations of flat panel imaging devices used in image-guided ion beam therapy *Phys. Med. Biol.* **61** N592–605